J. Am. Soc. Mass Spectrom. (2019) 30:1895–1905
DOI: 10.1007/s13361-019-02259-7

FOCUS: HONORING HELMUT SCHWARZ'S ELECTION TO THE NATIONAL ACADEMY OF SCIENCES: RESEARCH ARTICLE

Co-adsorption of O_2 and C_2H_4 on a Free Gold Dimer Probed via Infrared Photodissociation Spectroscopy

Sandra M. Lang,[1,2] Thorsten M. Bernhardt,[1] Joost M. Bakker,[3] Bokwon Yoon,[2] Uzi Landman[2]

[1]Institute of Surface Chemistry and Catalysis, University of Ulm, Albert-Einstein-Allee 47, 89069, Ulm, Germany
[2]School of Physics, Georgia Institute of Technology, Atlanta, GA 30332-0430, USA
[3]Radboud University Institute for Molecules and Materials, FELIX Laboratory, Toernooiveld 7, 6525 ED, Nijmegen, Netherlands

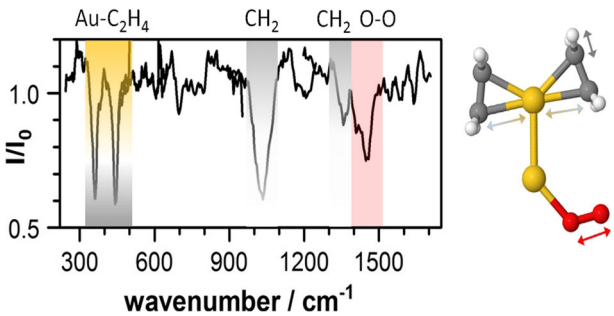

Abstract. Infrared multiple photon dissociation (IR-MPD) spectroscopy in conjunction with density functional theory (DFT) calculations has been employed to study the activation of molecular oxygen and ethylene co-adsorbed on a free gold dimer cation Au_2^+. Both studied complexes, $Au_2O_2(C_2H_4)^+$ and $Au_2O_2(C_2H_4)_2^+$, show distinct features of both intact O_2 and ethylene co-adsorbed on the cluster. However, the ethylene C=C double bond is activated, increasing in length by up to 0.07 Å compared with the free molecule, and the red shift of the O–O vibration frequency increases with the number of adsorbed ethylene molecules, indicating a small but increasing activation of the O–O bond. The small O_2 activation and the rather weak interaction between O_2 and C_2H_4 are also reflected in the calculated electronic structure of the co-adsorption complexes which shows only a small occupation of the empty anti-bonding O_2 $2\pi^*_{2p}$ orbital as well as the localization of most of the Kohn–Sham orbitals on O_2 and C_2H_4, respectively, with only limited mixing between O_2 and C_2H_4 orbitals. The results are compared with theoretical studies on neutral $Au_xO_2(C_2H_4)$ ($x = 3, 5, 7, 9$) complexes.

Keywords: Gold cluster, Ethylene oxidation, Vibrational spectroscopy, Density functional theory calculations, Gas phase reaction

Received: 6 March 2019/Revised: 4 May 2019/Accepted: 26 May 2019/Published Online: 12 July 2019

Introduction

The selective oxidation of hydrocarbons represents a central reaction in modern petroleum-based chemical industry [1]. One of the most important hydrocarbons is ethylene, C_2H_4, since it is used as a raw material for the synthesis of ethylene oxide (epoxide) and acetaldehyde and thus for the subsequent production of, e.g., polyesters, polyurethane, surfactants, detergents, anti-freeze, and food additives [2–5].

Industrially ethylene oxide is nowadays produced via direct oxidation of ethylene with molecular oxygen or air in the presence of an Ag/α–Al_2O_3 catalyst at about 470–570 K. To avoid the undesirable highly exothermic combustion of ethylene to CO_2, not only a highly selective catalyst but also an optimized process is needed. This can be achieved, e.g., by controlled heat removal, the addition of several promoters, and intentional poisoning of the catalyst [2–5]. With such an optimized process, a typical ethylene oxide selectivity of 70–83% can be achieved, which can be further increased to 90–93% by addition of NO_x to the feed gas [2]. However, due to the high costs of ethylene, even small further improvements of the catalyst selectivity are highly desirable.

So far, only silver-based materials have been identified as efficient and rather selective ethylene epoxidation catalysts.

Electronic supplementary material The online version of this article (https://doi.org/10.1007/s13361-019-02259-7) contains supplementary material, which is available to authorized users.

Correspondence to: Sandra Lang; *e-mail:* sandra.lang@uni–ulm.de

Despite long-standing and intense research, the mechanism underlying the industrial ethylene epoxidation reaction is still not completely understood. However, there is a general agreement that molecular oxygen is predissociated on the catalyst prior to reaction with ethylene. Thus, numerous studies discussed the importance of different oxygen species for product selectivity ([5–8] and references therein). Most other transition metals that easily dissociate molecular oxygen also activate and dissociate the ethylene C–H bond which leads to combustion rather than oxidation of ethylene, and consequently the literature on other metals for ethylene epoxidation catalysis is limited [8].

Promising alternative candidates might be small gold particles. Already two decades ago, Haruta and co-workers showed that gold nanoparticles with diameters smaller than 4 nm mediate the low-temperature oxidation of the alkene propylene with selectivities higher than 90% and conversions of 1–2% [9]. Furthermore, free gold clusters have been reported to activate the ethylene C=C double bond but to not affect the C–H bonds [10–16]. In addition, gold particles typically bind O_2 as intact molecules; thus, oxidation reactions mediated by gold clusters were shown to proceed via direct interaction of the reactants with molecular oxygen (for example, [17–22]) which opens up mechanistically completely new reaction pathways and enables low-temperature oxidation reactions. So far, however, studies on the ethylene oxidation mediated by gold surfaces and particles are scarce and mainly of theoretical nature.

The only experimental study on the potential thermally driven ethylene oxidation on gold surfaces dates back to 1986 and did not observe any reaction between ethylene and atomic oxygen on Au(110) [23]. For electrocatalytic oxidation of ethylene, an early experimental study using a gold electrode indicated the formation of a CH_3CH_2O intermediate [24] whereas a later study observed high product selectivity for acetaldehyde [25]. In marked contrast, gold nanoparticles supported on TiO_2 were found to be highly selective towards epoxide formation [26]. Most interestingly, all theoretical investigations of gold surfaces only considered the reaction of atomic instead of molecular oxygen with ethylene. The reaction typically proceeds via an oxametallacycle (OMC, Me–$C(H_2)C(H_2)$O–Me with Me denoting metal atoms) intermediate which represents the precursor for subsequent epoxide and acetaldehyde formation. For all studied surfaces, acetaldehyde formation was found to be both thermodynamically and kinetically favorable over ethylene oxide formation [7, 8, 27, 28]. Based on density functional theory (DFT) calculations, two mechanisms were identified which determine the catalyst selectivity towards ethylene oxide: For the OMC to transform to epoxide instead of acetaldehyde, the C–metal bond must be weaker than the O–metal bond and the formed epoxide must be stabilized against the adsorbed acetaldehyde [29].

In contrast to the surface studies, the interaction of ethylene with molecular oxygen has been investigated in the presence of gold nanoparticles, clusters, and atoms. For example, prismatic shaped Au_5 was found to be not a good oxidation catalyst since the reaction is kinetically unfavorable due to the weak binding of O_2 to Au_5 [30]. Employing the dipped adcluster model with Au_2O_2 and Au_4O_2 as adclusters, superoxide O_2^- formation has been identified as a crucial prerequisite for ethylene oxidation [31]. It was suggested that gold may function as a good oxidation catalyst when superoxide species can be formed and stabilized, which is however not possible on extended gold surfaces. The importance of O–O bond activation has also been addressed in theoretical explorations of the hexagonal fcc(111)-like and square fcc(100)-like faces of a neutral Au_{38} cluster as catalytically active sites [32], as well as of defect-stabilized Au atoms on graphene [33]. Furthermore, co-adsorbed additional ethylene or CO has been shown to serve as a promoter for O–O bond cleavage and thus for considerable reduction of activation barriers [34]. Similarly, theoretical studies of the O_2/C_2H_4 co-adsorption of a series of neutral gold clusters Au_x ($x = 1–9$) have predicted the ability of ethylene to promote the dissociation of O_2 [35, 36].

In this contribution, we present the first experimental investigation of the interaction of molecular oxygen and ethylene in the presence of a small well-defined gold cluster, Au_2^+. By employing infrared multiple photon dissociation (IR-MPD) spectroscopy in conjunction with DFT calculations, we investigate the co-adsorption complexes $Au_2O_2(C_2H_4)^+$ and $Au_2O_2(C_2H_4)_2^+$ in comparison with $Au_2O_2^+$ and $Au_2(C_2H_4)_z^+$ ($z = 1, 2$). Both co-adsorption complexes show distinct features of intact O_2 and ethylene and do not indicate the formation of oxidation products. Although the O–O bond activation is shown to increase with the number of co-adsorbed ethylene molecules, the activation is most likely too small to enable room-temperature oxidation reactions.

Methods

Experimental Methods

The experiments were carried out using a molecular beam apparatus and the Free Electron Laser for Intra-Cavity Experiments (FELICE) as described elsewhere [37, 38]. Briefly, cationic gold clusters were produced by pulsed laser ablation of a gold target in the presence of a short pulse of helium carrier gas seeded with about 5% oxygen. $Au_x(C_2H_4)_z^+$ and $Au_xO_2(C_2H_4)_z^+$ complexes were formed by introducing a mixture of 1% ethylene in helium via a second pulsed valve in an adjacent flow tube reactor. The cluster source and the flow tube reactor were held at room temperature during the experiment. After expansion of the reaction mixture, the formed molecular beam interacted with the IR laser beam of FELICE (spectral range of 245–1700 cm^{-1}, spectral width of approximately 0.4% FWHM of the central frequency, and 9-μs-long macropulse consisting of 1-ns-spaced micropulses). Sequential absorption of multiple IR photons led to the heating and fragmentation of the complex. IR-MPD spectra were recorded by measuring the cluster complex intensity I in the mass spectrum as a function of the IR frequency. For reference, mass spectra without IR radiation were recorded in between successive IR laser shots,

yielding a reference cluster complex intensity I_0. After interaction with FELICE, the ion beam was mass-analyzed with a reflectron time-of-flight mass spectrometer (estimated mass resolution of 800–1000 in the mass range of the Au_2^+ cluster complexes).

Theoretical Methods

The theoretical calculations were performed by using the Vienna ab initio simulation package (VASP) [39–42]. The wave functions were expanded in a plane wave basis with a kinetic energy cut-off of 400 eV. The interaction between the atom cores and the valence electrons was described by the projector augmented wave (PAW) potential [43], and the exchange-correlation potential by the PBE generalized gradient approximation (GGA) [44]. To minimize the electrostatic interaction with the images, a supercell with a lattice constant of 25 Å was used and a neutralizing background charge and dipole and quadrupole corrections to the total energy were applied [45].

The wave function character was evaluated by projecting them onto spherical harmonics (in particular l = 0, 1, 2) within spheres around each atom (angular momentum projected local density of states (PLDOS)). The radius of the spheres was chosen as the half the average bond length (covalent radius) and amounted to 1.36 Å (Au), 0.76 Å (C), and 0.31 Å (H) [46]. The density of states (DOS) shown in Figure 2 is the sum of the projected contributions (l = 0–2) calculated for each of the involved atoms.

The vibrational spectra of the cluster complexes were calculated in the harmonic approximation by determining the dynamical matrix (matrix containing the electron density response to atomic displacements from equilibrium) using density functional perturbation theory [47, 48] (see Table 1 in the supporting information for level of accuracy achieved in our calculations). No frequency scaling was applied, except for the O_2 stretch vibration as discussed below.

Results and Discussion

Adsorption of O_2 on Gold Clusters

The interaction between gold clusters and molecular oxygen has been studied intensively before. The adsorption of O_2 on gold clusters is chiefly governed by the mixing of the half-occupied anti-bonding π^*_{2p} orbitals of O_2 with the s-type orbitals of the gold cluster [49, 50]. Due to the $5d^{10}6s^1$ electron configuration of the gold atom, this leads to a pronounced odd-even alternation in the reactivity of gold anions with clusters comprising an even number of Au atoms (and thus one unpaired electron) being reactive and those comprising an odd number of Au atoms (and thus a spin-paired electron configuration) being non-reactive [51–56]. In contrast, cationic gold clusters were not found to react with molecular oxygen under thermal conditions down to 100 K [21, 51, 57, 58], and the reaction with O_2 was only observed if oxygen was added to the strong non-thermal laser plasma of a laser ablation source [59] or after preadsorption of electron-donating reactants such as H_2, N_2, and CH_4 [20, 21, 60]. However, a few years ago, Woodham and Fielicke reported on the preparation of $Au_x(O_2)_y^+$ ($x = 2$–25) complexes at about 210 K in a flow tube reactor [61]. Subsequent IR-MPD spectroscopy of some of the formed complexes revealed that Au_{10}^+ and Au_{22}^+ even bind a first O_2 molecule in a superoxo state, whereas Au_4^+ and Au_{21}^+ physisorb a first O_2 molecule, and superoxo species are only observed upon adsorption of multiple O_2 molecules.

In the present study, we have produced $Au_2O_2^+$ by introducing O_2 to the He carrier gas of the laser ablation source; thus, the reaction occurred under non-thermal conditions. Previous experiments showed that this approach can lead to the formation of $Au_xO_y^+$ ($x = 1$–4, $y = 1$–8), i.e., O_2 can dissociate most likely during the laser vaporization process [62]. Our mass spectra show that $Au_xO_y^+$ with an odd number of O atoms are only produced in a small amount indicating that O_2 dissociation in the cluster source only represents a minor process. Furthermore, Figure 1 a displays the IR-MPD spectrum of $Au_2O_2^+$ clearly showing the O–O stretch vibration as a depletion of the ratio I/I_0 at 1503 cm^{-1}. The very weak signal around 1370 cm^{-1} was not observed in repeated measurements under slightly different conditions and is thus regarded as noise instead of a real signal. This demonstrates that in $Au_2O_2^+$ oxygen is physisorbed as an intact O_2 molecule and the O–O bond is only slightly activated (compare 1503 cm^{-1} with 1580 cm^{-1} of the free O_2 molecule [63]). Superoxide formation as, e.g., reported for Au_{10}^+ is not observed for the gold dimer.

Figure 1 b displays the corresponding calculated vibrational spectrum for $Au_2O_2^+$ (iso 2,1,0). The O–O stretch vibration is calculated to be 1472 cm^{-1} which we interpret as a slight overestimation of the weak gold–oxygen interaction, although it should be noted that the same method also slightly overestimates (by < 1%, see Table 1 in the supporting information, SI) the free O_2 stretch vibration. To compensate for this discrepancy between the experimental and theoretical O–O stretch vibration of about 30 cm^{-1}, we introduce a scaling factor of 1.021 for the O–O stretch. This scaling factor will in the following be applied to all O–O stretch frequencies while all other modes remain unscaled.

The calculated spectrum shows two further modes at 383 cm^{-1} and 211 cm^{-1} which can be assigned to two bending-like Au–O_2 modes (for details see Figure S2 in the supporting information). Both modes could not be directly observed in the experiment since in this region the spectrum of $Au_2O_2^+$ is contaminated by fragmentation of $Au_2(O_2)_2^+$ into the $Au_2O_2^+$ mass channel which appears as a signal $I/I_0 > 1$ centered at 323 cm^{-1} and 244 cm^{-1}. However, the calculated spectra of $Au_2O_2^+$ and $Au_2(O_2)_2^+$ show that these vibrations have similar eigenfrequencies for both complexes (see Figure S2 in the supporting information). Although we have no direct experimental evidence, it appears plausible to conclude that the overestimation of the gold–oxygen interaction in $Au_2O_2^+$ leads not only to a red shift of the O–O stretch mode by about 30 cm^{-1} but also to a blue shift of the higher-energy Au–O_2 bending-like mode (theoretically predicted at 383 cm^{-1}) of

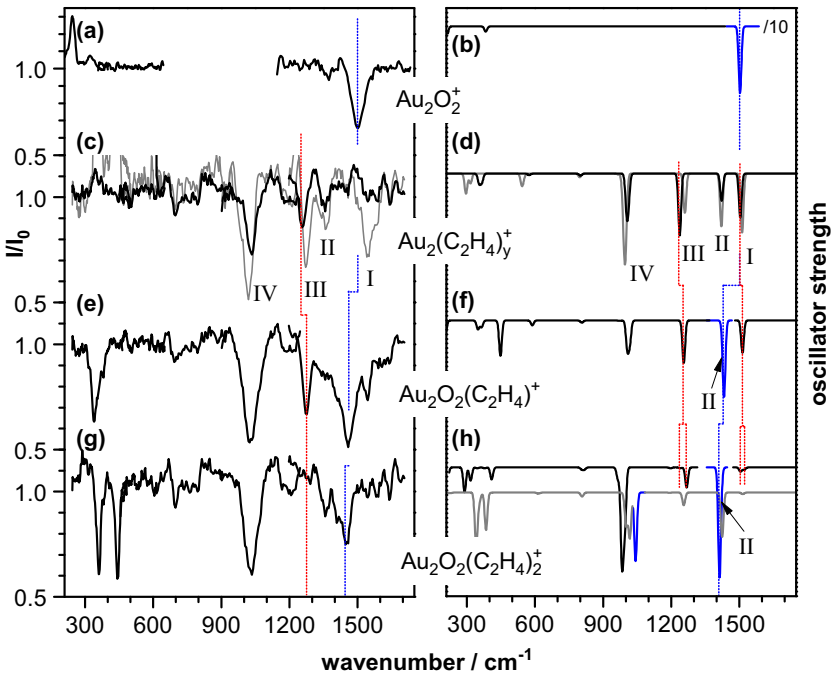

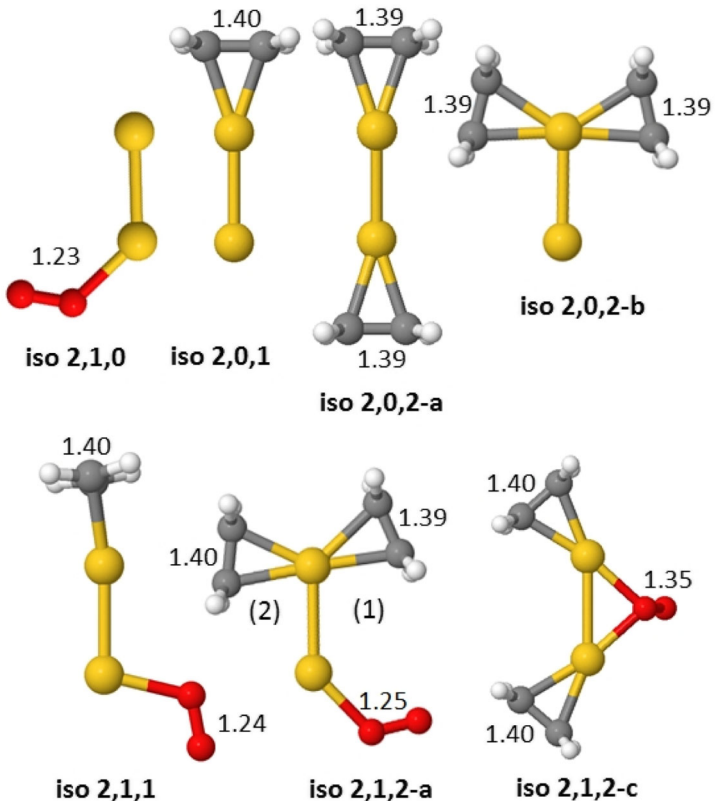

Figure 1. Experimental IR-MPD (left column) and calculated vibrational spectra (right column) of (**a**, **b**) $Au_2O_2^+$, (**c**, **d**) $Au_2(C_2H_4)^+$ (black curves) and $Au_2(C_2H_4)_2^+$ (gray curves) [10], (**e**, **f**) $Au_2O_2(C_2H_4)^+$, and (**g**, **h**) $Au_2O_2(C_2H_4)_2^+$. Panel (**h**) shows the calculated spectra of iso 2,1,2-a (black curve) and iso 2,1,2-c (gray curve). The gray curve has been shifted for the sake of clarity. The calculated spectra are convoluted with a 20 cm^{-1} FWHM Gaussian line shape function and are all shown on the same scale. The intensity of the O–O stretch mode (blue curve) has been divided by a factor of 10 in all spectra, except in the one of 2,1,2-c. The structures corresponding to the calculated spectra are shown at the bottom and are discussed in the text. The labels iso *x*,*y*,*z* correspond to $Au_x(O_2)_y(C_2H_4)_z^+$. Au, O, C, and H atoms are depicted by yellow, red, gray, and white spheres. The numbers give the C=C and O–O bond length in Å

at least 50 cm^{-1}. In marked contrast, the lower-energy Au–O_2 bending-like mode (theoretically predicted at 244 cm^{-1}) seems red-shifted although it appears to be rather insensitive to the gold–oxygen interaction (see also discussion below for the complexes $Au_2O_2(C_2H_4)^+$ and $Au_2O_2(C_2H_4)_2^+$). We can thus not decisively conclude whether these frequency mismatches are solely due to a mismatch in the Au_2^+–O_2 interaction or also due to possible shallowness of the binding potential. Details on the electronic structure of $Au_2O_2^+$ are given in the supporting information.

IR-MPD Spectra of $Au_2(C_2H_4)_z^+$ (z = 1, 2) Complexes

In a recent IR-MPD spectroscopic and theoretical investigation of $Au_x(C_2H_4)_z^+$, we have shown that up to three C_2H_4 molecules bind to gold cations in a π-bonded configuration [10], in agreement with previous theoretical studies [11, 14, 16]. The interaction of gold clusters with ethylene is governed by mixing of the ethylene C=C bond–forming orbitals σ_{CC} and π_{CC} with gold orbitals. This leads to a net electron charge donation from ethylene to the gold cluster and an activation of the C=C double bond, whereas the C–H bond is not affected.

For comparison, Figure 1 c displays the IR-MPD spectra of the gold dimer complexes $Au_2(C_2H_4)^+$ (black curve) and $Au_2(C_2H_4)_2^+$ (gray curve) [10]. The experimentally observed bands labeled I to IV are in agreement with the calculated vibrational spectra (Figure 1d) of the π-bonded minimum energy structures (iso 2,0,1 and iso 2,0,2-a). Bands I and III correspond to coupled C=C stretch/in-plane CH_2 scissor motions, band II can be assigned to CH_2 scissor motions, and band IV to CH_2 wagging motions. In very good agreement with the experimental data, band III slightly blue-shifts (experimental 19 cm^{-1}, theoretical 23 cm^{-1}) upon adsorption of a second ethylene molecule, indicating a small deactivation of the C=C bond, and band IV slightly red-shifts (experimental 15 cm^{-1}, theoretical 14 cm^{-1} and 11 cm^{-1}), whereas the spectral position of band II appears to be independent of the number of adsorbed C_2H_4 molecules on the cluster. Furthermore, band I is theoretically predicted to blue-shift by 8 cm^{-1}, an effect that cannot be observed in the IR-MPD spectrum due to the small signal intensity of the experimental band I.

As discussed previously [10], the similarity of the vibrational frequencies of both bands I and II for the di- and mono-ethylene complexes most likely leads to a cancelation of the signal in the IR-MPD spectrum of $Au_2(C_2H_4)^+$ via fragmentation of $Au_2(C_2H_4)_2^+$ into the mass channel of $Au_2(C_2H_4)^+$ and can thus explain the very weak bands I and II in the spectrum of $Au_2(C_2H_4)^+$. It should be noted that the calculated frequencies of bands I, III, and IV and even their relative spectral shifts going from $Au_2(C_2H_4)^+$ to $Au_2(C_2H_4)_2^+$ are in favorable agreement with the experimentally observed frequencies. In contrast, the calculated frequency of band II is consistently overestimated by about 60–70 cm^{-1} for all investigated complexes, $Au_2(C_2H_4)_z^+$ and $Au_2O_2(C_2H_4)_z^+$ (see also discussion below).

In our previous study, we found a second isomer (iso 2,0,2-b) with both ethylene molecules π-bonded to the same Au atom. This isomer is 0.33 eV higher in energy but has a very similar vibrational spectrum and cannot be distinguished from the minimum energy structure on the basis of the IR-MPD spectrum.

IR-MPD Spectra of $Au_2O_2(C_2H_4)_z^+$ (z = 1, 2) Co-adsorption Complexes

In order to gain insight into the interaction between ethylene and molecular oxygen, we have next studied the co-adsorption complexes $Au_2O_2(C_2H_4)^+$ and $Au_2O_2(C_2H_4)_2^+$. Figure 1 e displays the IR-MPD spectrum of $Au_2O_2(C_2H_4)^+$ which exhibits all features of the above discussed complex $Au_2(C_2H_4)^+$, which we will continue to refer to as bands I–IV, as well as a relatively intense band centered at 1458 cm^{-1} that is assigned to the O–O stretch vibration of molecular oxygen. Compared with $Au_2O_2^+$, the O–O stretch vibration is red-shifted from 1503 to 1458 cm^{-1} indicating a slightly increased O–O bond activation. Furthermore, compared with $Au_2(C_2H_4)^+$, band III is somewhat blue-shifted by about 15 cm^{-1} whereas the spectral position of band IV and most likely also of band II is not affected. The low intensity of band I of $Au_2(C_2H_4)^+$ renders any conclusions about this band difficult. Besides, a new band at 346 cm^{-1} is observed.

This IR-MPD spectrum is consistent with the calculated spectrum (Figure 1f) of the minimum energy structure iso 2,1,1 in which O_2 and C_2H_4 are co-adsorbed at two different Au atoms. In particular, the predicted red shift of the O–O stretch vibration and the blue shift of band III are mirrored in the experimental spectrum. However, the experimental spectrum shows a red shift of the O–O stretch mode by 45 cm^{-1} (from 1503 for $Au_2O_2^+$ to 1458 cm^{-1} for $Au_2O_2(C_2H_4)^+$), whereas the calculations predict a red shift of 70 cm^{-1} (from 1503 for $Au_2O_2^+$ to 1432 cm^{-1} for $Au_2O_2(C_2H_4)^+$) which indicates that the weak gold–oxygen bond is even more overestimated in the co-adsorption complex. Furthermore, the predicted intensity of band III, especially relative to that predicted for band IV, is overestimated. This band was already weak in the experimental spectrum of $Au_2(C_2H_4)^+$, likely due to (partial) signal canceling resulting from fragmentation of $Au_2(C_2H_4)_2^+$ complexes, and such a scenario could also play a role here. As described above, mode II is consistently blue-shifted by 60–70 cm^{-1} in all calculated spectra and is thus hidden in the red edge of the strong O–O stretch band (marked by an arrow). Furthermore, the theoretical spectrum predicts a small blue shift of band I by 10 cm^{-1}.

At the red end of the spectrum, the calculations predict four modes at 448, 365, 349 cm^{-1}, and 205 cm^{-1} which correspond to the Au–O_2 bending-like motions and the asymmetric and symmetric Au–C_2H_4 stretch modes, respectively. In contrast, the experimental spectrum shows only one band centered at 346 cm^{-1}. It appears safe to assign this to the theoretically predicted symmetric and asymmetric Au–C_2H_4 stretch modes, even though their predicted intensities are lower than the

higher-energy Au–O_2 bending-like mode. The apparent absence of the latter in the experimental spectrum might be explained by the already discussed overestimation of the weak gold–oxygen interaction, which for $Au_2O_2^+$ led to a red shift of at least 50 cm^{-1}. Considering the even more pronounced overestimation of the gold–oxygen bond in $Au_2O_2(C_2H_4)^+$, it seems reasonable to assume that this mode is even further red-shifted from the predicted 448 cm^{-1} and that it might overlap with the Au–C_2H_4 stretch modes. We thus interpret the band observed at 346 cm^{-1} as due to an overlap of the Au–O_2 bending-like and Au–C_2H_4 stretch modes. The lower-energy Au–O_2 bending-like mode (theoretically predicted at 205 cm^{-1}) is most likely shifted out of the probed spectral region.

Figure 1 g shows the IR-MPD spectrum recorded for the $Au_2O_2(C_2H_4)_2^+$ mass channel. This spectrum also shows a double peak in the spectral region of 1300–1500 cm^{-1} which might be attributed to a slightly red-shifted (by about 17 cm^{-1} to 1441 cm^{-1}) O–O stretch mode and band II of π-bonded ethylene, although the total depletion is less than for $Au_2O_2(C_2H_4)_2^+$. Bands I and III are no longer discernible in the spectrum, whereas bands II and IV appear largely unaffected. In contrast to $Au_2O_2(C_2H_4)^+$, the low wavenumber region of the spectrum now exhibits two intense modes at 361 cm^{-1} and 443 cm^{-1}, respectively.

This spectrum is in reasonable agreement with the calculated vibrational spectrum (cf. Figure 1h) of a complex with the two ethylene molecules adsorbed on the same Au atom and the O_2 molecule co-adsorbed on the second Au atom (iso 2,1,2-a). In particular, this spectrum shows a strongly reduced oscillator strength for modes I and III which can explain their absence in the experimental spectrum. It also nicely reproduces the shift in the O–O stretch mode (experimental 17 cm^{-1}, theoretical 20 cm^{-1}). Similar to $Au_2O_2(C_2H_4)^+$, band II is hidden under the O–O stretch mode and is marked by an arrow. The predicted intensity for the O–O stretch vibration is, however, not reduced, leaving the reduced depletion intensity unexplained, potentially hinting at the presence of another isomer. At the red end of the spectrum, four modes at 409, 317, 290, and 214 cm^{-1} are predicted which correspond to the Au–O_2 bending-like modes as well as the symmetric Au–C_2H_4 stretch modes of the two ethylene molecules. If we again assume that the Au_2^+–O_2 bending-like vibration has been overestimated, the 409cm $^{-1}$ band can either overlap with the band at 361 cm^{-1} or even shift out of the probed spectral window. Although somewhat red-shifted, the remaining modes predicted at 317 cm^{-1} and 290 cm^{-1} could then explain the presence of the experimental bands at 443 cm^{-1} and 361 cm^{-1}. The asymmetric Au–C_2H_4 stretch modes have frequencies of 379 and 346 cm^{-1} but only very small oscillator strengths and are thus not visible in the IR-MPD and the theoretical vibrational spectrum.

Most interestingly, the above-described isomer of $Au_2O_2(C_2H_4)_2^+$ does not represent the minimum energy structure. We have found three isomers 0.49 eV (iso 2,1,2-b), 0.46 eV (iso 2,1,2-c), and 0.38 eV (iso 2,1,2-d) lower in energy, respectively, in which the C_2H_4 molecules bind to two different Au atoms (cf. Figure S4 in the supporting information). The O_2 molecule is either η^1- or η^2-bonded to a C_2H_4-binding Au atom or bridge-bonded between the two Au atoms. η^1- and η^2-binding lead to a considerable red shift of the O–O stretch vibration (relative to free O_2) by about 345 cm^{-1} and 360 cm^{-1}, respectively, bringing it down to 1230 cm^{-1}, effectively ruling out their presence as no intense depletion is observed here.

In contrast, in the bridge-bonded isomer, the O–O stretch vibration couples with C_2H_4 modes and is even further red-shifted by about 540 to 1042 cm^{-1}, almost overlapping band IV of the π-bonded ethylene (see gray spectrum in Figure 1h). In addition, iso 2,1,2-c has strong low-frequency bands centered at 386 cm^{-1} (arising from three modes: the low intensity Au–O_2 stretch mode and the two asymmetric Au–C_2H_4 stretch modes) and 342 cm^{-1} (two symmetric Au–C_2H_4 stretch modes and a Au–O_2 rocking-like mode). At first glance, these modes could better account for the two bands observed in the low-energy part of the IR-MPD spectrum than iso 2,1,2-a, although the frequency mismatch between observed and predicted band maxima is still considerable. It would thus be tempting to assign the experimental spectrum as solely due to iso 2,1,2-c were it not for the double peak structure in the 1300–1500 cm^{-1} range: if we assume the low-frequency component is invariably assignable to the ethylene CH_2 scissor motion (assuming a consistent theoretical overestimation of band II by 60–70 cm^{-1} as found for $Au_2(C_2H_4)_{1,2}^+$ and $Au_2O_2(C_2H_4)^+$), iso 2,1,2-c can only account for this band and not for the more intense band with a maximum at 1450 cm^{-1}. With its only moderately red-shifted O–O stretch mode, iso 2,1,2-a offers a plausible explanation for this band. We thus tentatively assign the IR-MPD spectrum to a combination of isomers iso 2,1,2-c and iso 2,1,2-a and speculate that the presence of a higher-energy isomer iso 2,1,2-a is due to kinetic trapping of an entrance complex, where the second ethylene preferably adsorbs on the Au atom already binding the first ethylene. A bridge-bound isomer for $Au_2O_2(C_2H_4)^+$ was considered computationally, but this proved unstable, consistently converging to a structure where O_2 and ethylene adsorb on opposite Au atoms.

To summarize, the IR-MPD spectra of the co-adsorption complexes $Au_2O_2(C_2H_4)^+$ and $Au_2O_2(C_2H_4)_2^+$ show distinct features of both intact O_2 and ethylene co-adsorbed on the cluster. Despite the observation of intact O_2 and C_2H_4, the continuous red shift of the O–O vibration going from iso 2,1,1-a to iso 2,1,2-a indicates an increasing activation of the O–O bond due to the co-adsorption of ethylene molecules (the bridge-bound O_2 in iso 2,1,2-c obviously is much more strongly affected). Furthermore, modes I and III are shown to blue-shift upon co-adsorption of a second ethylene molecule or O_2 on $Au_2(C_2H_4)^+$. Since these modes correspond to a mixed C=C stretch/in-plane CH_2 scissor motion, this indicates a slight deactivation of the C=C bond.

C–C, C–H, and O–O Bond Activation

To gain further insight into the mutual activation of the O–O bond and the deactivation of the C=C bond upon co-adsorption of O_2 and C_2H_4 on Au_2^+, we have theoretically studied the geometric and electronic structure of the complexes $Au_2O_2(C_2H_4)^+$ and $Au_2O_2(C_2H_4)_2^+$ in more detail.

Recently, we have theoretically investigated the structure of the complex $Au_2(C_2H_4)^+$ and showed that adsorption of one ethylene molecule on the cluster leads to an elongation of the C=C bond from 1.33 for the free C_2H_4 molecule (1.34 Å experimental value [64]) to 1.40 Å in $Au_2(C_2H_4)^+$ (cf. iso 2,0,1) [10]. Co-adsorption of O_2 on the free (i.e., non-ethylene binding) Au atom slightly reduces the C=C bond length (< 0.01 Å compared with ethylene in $Au_2(C_2H_4)^+$) accompanied by a small elongation of the calculated O–O bond length (0.01 Å compared with free O_2). Although these bond length changes are very small, they are reflected in the vibrational spectra: bands I and II corresponding to coupled C=C stretch/in-plane CH_2 scissor motions slightly blue-shift (cf. Figure 1e, f) and the O–O stretch vibration red-shifts from 1580 (free O_2) to 1458 cm^{-1} ($Au_2O_2(C_2H_4)^+$). Furthermore, O_2/C_2H_4 co-adsorption on Au_2^+ leads to a slight shortening of the Au–Au bond from 2.62 of the bare Au_2^+ to 2.60 Å in the co-adsorption complex.

As described above, the IR-MPD spectrum of $Au_2(C_2H_4)_2^+$ is in reasonable agreement with the calculated spectrum of the minimum energy structure (iso 2,0,2-a) in which each ethylene molecule is bound to one of the Au atoms in a π-bonded configuration. In this complex, the C=C bond lengths of both molecules amount to 1.39 Å, which is slightly shorter than in $Au_2(C_2H_4)^+$ and is in agreement with the small blue shift of bands I and III. The isomer with both ethylene molecules π-bonded to the same Au atom (iso 2,0,2-b) is 0.33 eV higher in energy. The C=C bond length in this complex also amounts to 1.39 Å, and the vibrational spectrum is very similar to the spectrum of iso 2,0,2-a.

The IR-MPD spectrum of $Au_2O_2(C_2H_4)_2^+$ is tentatively assigned to two species. One of these is iso 2,1,2-a, which corresponds to the co-adsorption of O_2 on iso 2,0,2-b. This leads to an elongation of the Au–Au bond to 2.69 Å (compare with 2.62 Å for Au_2^+), the O_2 orientation in this structure breaks the symmetry, and the two ethylene molecules no longer occupy equivalent sites leading to a splitting of bands I and III. The C_2H_4 molecule closer to the O_2 molecule (labeled (1) in Figure 1) is characterized by a C=C bond length of 1.39 Å and is thus hardly affected by the O_2 molecule. The corresponding bands I and III are theoretically predicted at 1521 cm^{-1} and 1268 cm^{-1}, respectively, similar to bands I and III of $Au_2(C_2H_4)_2^+$ at 1512 cm^{-1} and 1260 cm^{-1} (d(C=C) = 1.39 Å). In contrast, the C_2H_4 molecule more distant to O_2 (labeled (2) in Figure 1) is slightly activated to d(C=C) = 1.40 Å with bands I and III predicted at 1505 cm^{-1} and 1240 cm^{-1}, respectively, similar to bands I and III of $Au_2(C_2H_4)^+$ at 1504 cm^{-1} and 1237 cm^{-1} (d(C=C) = 1.40 Å). However, due to the small oscillator strengths of these modes, they are not observed in the experimental spectrum. In addition, the co-adsorption of O_2 on $Au_2(C_2H_4)_2^+$ leads to a further small activation of the O–O bond to 1.25 Å compared with 1.23 Å in free O_2 and 1.24 Å in $Au_2O_2(C_2H_4)^+$ in agreement with the observed red shift of the O–O stretch vibration to 1441 cm^{-1}. For none of the investigated complexes, any C–H bond activation is observed (compare d(C–H) = 1.09 Å in $Au_2(C_2H_4)_z^+$ and $AuO_2(C_2H_4)_z^+$ with d(C–H) = 1.09 Å in free C_2H_4).

The second isomer tentatively assigned, iso 2,1,2-c, corresponds to co-adsorption of O_2 on iso 2,0,2-a by bridging the two Au atoms. This leads to a rotation of the C_2H_4 molecules and a considerable elongation of the Au–Au bond to 2.88 Å (compare with 2.62 Å in Au_2^+). Both ethylene molecules are slightly activated to d(C=C) = 1.40 Å, and the O–O bond is considerably elongated to 1.35 Å. This is consistent with the strong red shift of the O–O stretch mode by about 540 cm^{-1}.

Electronic Structure of $Au_2O_2(C_2H_4)_z^+$ Complexes

Despite the observed O–O and C=C bond activation processes, the O_2 activation is rather small and the IR-MPD spectra are well-described by simple co-adsorption products without any indication for further C–O or O–H bond formation reactions. To understand this weak O_2/C_2H_4 interaction, Figure 2 displays the electronic density of states (DOS) for $Au_2O_2(C_2H_4)^+$ and $Au_2O_2(C_2H_4)_2^+$ (iso 2,1,2-a) together with selected Kohn–Sham (KS) orbitals. The DOS are shown separately for spin-up (majority spin) and spin-down (minority spin) electrons. The features colored red correspond to electron occupation localized on the O_2 molecule, the green features to the sum of charges localized on the C_2H_4 and the O_2 molecule, and the gray features represent the total DOS. For both complexes, the low-lying orbitals closely resemble the orbitals σ_{2s}, σ^*_{2s}, σ_{2p}, and π_{2p} of free O_2 as well as the C–H bond–forming orbitals σ^+_{CH2}, σ^-_{CH2}, π^+_{CH2}, and π^-_{CH2} of the free ethylene molecule, i.e., these orbitals are localized on the O_2 and C_2H_4 molecules, respectively. Similar to the previously studied complex $Au_2(C_2H_4)^+$ [10], the ethylene C=C double bond–forming orbitals σ_{CC} and π_{CC} for $Au_2O_2(C_2H_4)^+$ and $Au_2O_2(C_2H_4)_2^+$ mix with the Au_2^+ d-orbitals leading to a partial depopulation of the π_{CC} and an elongation of the C=C double bond by up to 0.07 Å compared with the free ethylene molecule [10]. Since all CH_2 bond–forming orbitals are localized on the C_2H_4 molecule and do not mix with gold orbitals, the ethylene C–H bonds are not activated compared with free ethylene.

The anti-bonding π^*_{2p} orbitals of O_2 close to the Fermi energy (ε_F) are occupied forming the orbitals labeled #22 and #23 for $Au_2O_2(C_2H_4)^+$ and #28 and #29 for $Au_2O_2(C_2H_4)_2^+$. Whereas orbitals #22 and #29 are of bonding nature between O_2 and Au_2^+, orbitals #23 and #28 are mainly localized on the O_2 molecule. The highest occupied molecular orbital (HOMO) is formed by interaction of the Au_2^+ 1S superatom-like orbital [65] with one of the unoccupied O_2 orbitals. This pulls part of the initially unoccupied π^*_{2p} orbitals below the Fermi level leading to a partial occupation of the orbital and an activation of the O–O bond. However, since this contribution to the HOMO is rather small, i.e., most of the initially unoccupied

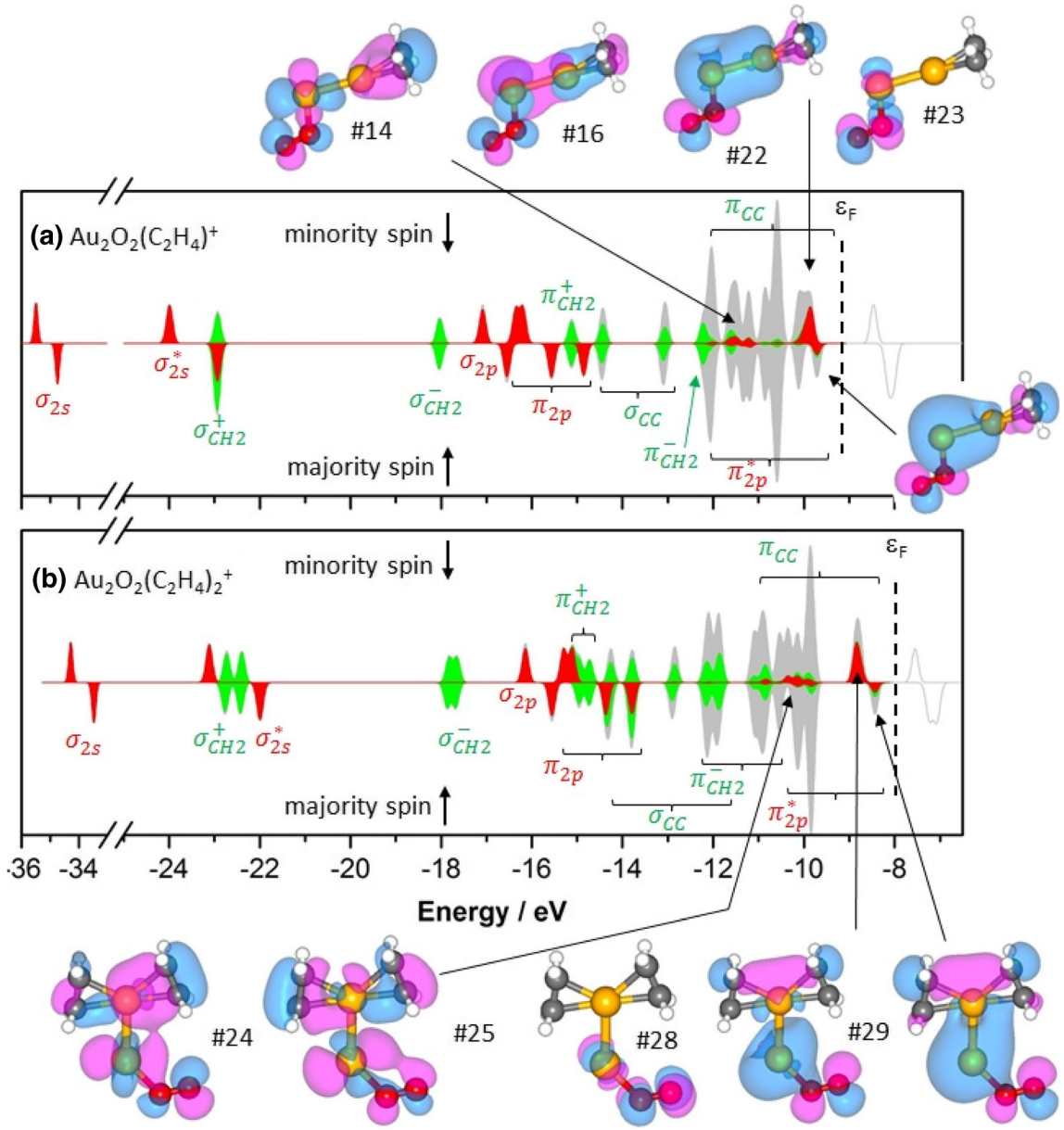

Figure 2. Electronic structure, represented by the density of states (DOS) and isosurfaces (encompassing 90% of the electron density) of selected Kohn–Sham orbitals (with positive and negative values depicted in blue and pink, respectively) for (**a**) $Au_2O_2(C_2H_4)^+$ and (**b**) $Au_2O_2(C_2H_4)_2^+$. The DOS is shown separately for spin-up and spin-down electrons. For occupied states (energy below the Fermi level ε_F, vertical dashed line), the area under the DOS curve is filled. The red features correspond to the electronic states (charge) localized on the O_2 molecule, the green features to the charge localized on the C_2H_4 and the O_2 molecules, and the gray curve represent the total DOS

π^*_{2p} orbitals are still located above ε_F, the activation of the O–O bond is rather small, reflected by an elongation of only 0.01 Å for $AuO_2(C_2H_4)^+$ and 0.02 Å for $AuO_2(C_2H_4)_2^+$ and a rather small red shift of the O–O stretch vibration (122 cm^{-1} and 139 cm^{-1}, respectively). The interaction of the cationic gold cluster with O_2 is similar to the previously reported interaction of neutral gold clusters with O_2 but different to $Au_xO_2^-$ for which the gold–O_2 interaction is governed by a considerable occupation of the initially unoccupied π^*_{2p} orbitals [49].

Furthermore, some peaks of the $Au_2O_2(C_2H_4)^+$ and $Au_2O_2(C_2H_4)_2^+$ DOS (in particular between − 12 and − 9 eV) show (at least small) contributions of both O_2 and C_2H_4. However, the corresponding KS orbitals (e.g., the orbitals labeled #14 and #16 for $Au_2O_2(C_2H_4)^+$ and #24 and #25 for $Au_2O_2(C_2H_4)_2^+$) do not indicate any noticeable mixing of O_2 and C_2H_4 orbitals but rather represent multi-centered orbitals. Thus, the localization of most of the KS orbitals on O_2 and C_2H_4, respectively, the small contribution of the initially unoccupied π^*_{2p} orbital to the HOMO, and the limited mixing between O_2 and C_2H_4 orbitals are responsible for the rather weak interaction and mutual activation between the co-adsorbed molecules.

O_2/C_2H_4 Co-adsorption on Neutral Gold Clusters

The mutual activation of O_2 and C_2H_4 mediated by neutral gold clusters has been investigated previously by means of DFT calculations. Small neutral gold clusters with an odd number of atoms Au_x ($x = 3–9$; i.e., with one unpaired s-electron) were found to activate one oxygen molecule to a superoxo state (d(O–O) = 1.28–1.31 Å) [35] which represents a considerably stronger activation than observed for Au_2^+ in the present study. Despite the strong activation of O_2, molecular adsorption of O_2 has been found to be thermodynamically favorable over dissociative adsorption (with the exception of Au_9) which appears to be in contrast to an earlier study on neutral Au_xO_2 complexes [49]. Similar to Au_2^+, a first ethylene molecule binds to the neutral cluster in a π-configuration (with the exception of Au_5) and the C=C bond is elongated to about 1.38–1.39 Å [11] and 1.41–1.43 Å [12], respectively.

Co-adsorption of one O_2 and one C_2H_4 molecule has been shown to be slightly cooperative, i.e., the energy of simultaneous adsorption of both molecules is 0.05–0.1 eV larger than the sum of the individual adsorption energies [35]. Most interestingly, co-adsorption of C_2H_4 on Au_xO_2 has been found to hardly influence the charge transfer to the molecularly adsorbed O_2 molecule [36], and consequently, the change of O–O bond activation upon C_2H_4 co-adsorption is very small. A similar small ethylene-induced O–O bond activation is also observed in the IR-MPD spectra of $Au_2O_2(C_2H_4)^+$ and $Au_2O_2(C_2H_4)_2^+$.

Despite the small O–O bond activation induced upon ethylene co-adsorption on neutral Au_xO_2, charge transfer processes have been shown to promote O_2 dissociation by energetically stabilizing the isomers with dissociated oxygen and thus considerably reducing the energy barrier for O–O bond dissociation [36]. Since the barriers are still around 1.0 eV, the adsorption of multiple ethylene molecules has been proposed to further decrease the barrier and to make the reaction feasible at low temperatures. However, several studies on oxidation reactions mediated by gold clusters such as the oxidation of CO [17, 18], methane [20], H_2 [21], and ethylene [31–33] showed that O_2 dissociation does not represent a necessary prerequisite for gold-mediated oxidation reactions. The molecules can rather interact with sufficiently activated but molecularly adsorbed O_2 which was shown to open mechanistically different reaction pathways and to enable low-temperature oxidation reactions. Consequently, not only the activation of O_2 but also the activation of the reaction partner might be crucial. In the previous sections, we have shown that adsorption of two ethylene molecules besides O_2 on Au_2^+ leads not only to the largest O_2 but also to the largest C=C bond activation. Thus, the adsorption of multiple ethylene molecules appears to lead to a cooperative effect resulting in maximal O_2 and C_2H_4 activation and could provide the necessary preconditions for any potential subsequent oxidation reactions.

However, due to the intrinsically weak interaction between the cationic gold cluster and molecular oxygen, this cooperative effect appears to be insufficient for any further C–O or O–H bond formation reactions. This is in agreement with the proposed necessity of a superoxide species for successful ethylene oxidation [31]. Neutral and anionic gold clusters have been shown to activate ethylene to a similar extent as gold cations [11, 12] but, with the exception of Au_{10}^+ and Au_{22}^+ [61], neutral and anionic gold clusters with one unpaired s-electron typically activate molecular oxygen considerably stronger [35, 49, 56, 61, 66–73]. Thus, neutral and anionic gold cluster are suggested to represent better candidates to mediate the oxidation of ethylene. The reaction might be energetically even more favorable in the presence of a cluster that preferably binds ethylene in a di-σ-bonded configuration instead of a π-bonded configuration. In the π-bonded configuration, the C atoms retain their sp^2 hybridization of the free C_2H_4 molecule while they are rehybridized to an almost sp^3-like state in the di-σ-bonded configuration leading to a considerably stronger activation of the C–C bond [11, 12, 15]. Since only for the neutral Au_5 cluster di-σ-bonding of ethylene has been shown to be energetically more favorable than π-bonding, Au_5 appears to be the most promising candidate to successfully mediate the direct oxidation of ethylene without predissociation of the O_2 molecule.

However, a recent theoretical study has shown that both epoxide and acetaldehyde formation are energetically more favorable with initially π-bonded ethylene [32]. Ethylene binds to the hexagonal fcc(111)-like face of a neutral Au_{38} cluster in a di-σ-bonded configuration leading to d(C–C) = 1.478 Å while O_2 adsorption on this face leads to an activation of the O–O bond to d(O–O) = 1.366 Å. Most interestingly, co-adsorption of both molecules on the same hexagonal face of Au_{38} results in a small deactivation of both molecules to d(C–C) = 1.463 Å and d(O–O) = 1.348 Å. In contrast, ethylene binds to the square fcc(100)-like face of the cluster in a π-bonded configuration with d(C–C) = 1.381 Å, and O_2 is activated on the same face to d(O–O) = 1.358 Å. Co-adsorption of both molecules does not affect the ethylene molecule (d(C–C) = 1.380 Å) but further activates the O–O bond to d(O–O) = 1.368 Å. The subsequent oxidation reactions to epoxide and acetaldehyde were then found to be energetically more favorable on the fcc(100)-like face with π-bonded ethylene. This shows that a strong activation of the O–O bond is more important for subsequent oxidation reactions than the activation of the C=C bond. Thus, ethylene oxidation should be most favorable in the presence of anionic gold cluster with an odd number of atoms.

Conclusion

We employed IR-MPD spectroscopy in conjunction with DFT calculations to investigate the activation of molecular oxygen and ethylene in the co-adsorption complexes $Au_2O_2(C_2H_4)^+$ and $Au_2O_2(C_2H_4)_2^+$. Both complexes show characteristic features of intact O_2 and C_2H_4 and do not indicate the formation of oxidation products. However, spectral shifts of the C=C and O–O stretch modes are observed which are in agreement with an activation of the C=C double bond by up to 0.07 Å and a small activation of the O–O bond by up to 0.02 Å which

increases with the increasing number of co-adsorbed ethylene molecules. The small O_2 activation and the rather weak interaction between O_2 and C_2H_4 are also reflected in the electronic structure of the co-adsorption complexes which shows only a small occupation of the empty anti-bonding O_2 $2\pi^*_{2p}$ orbital as well as the localization of most of the Kohn–Sham orbitals on O_2 and C_2H_4, respectively. This study shows that although the co-adsorption of ethylene molecules enhances the activation of the oxygen molecules, the cationic Au_2^+ cannot promote sufficient activation to enable room-temperature ethylene oxidation. To enhance the O_2 activation to a superoxo or peroxo state, larger gold cluster cations such as Au_{10}^+ and Au_{22}^+ [61] or anionic clusters with an odd number of gold atoms Au_x^- (x = odd number) [35, 49, 56, 67, 68, 70, 71] should be employed.

Acknowledgements

We gratefully acknowledge the Nederlandse Organisatie voor Wetenschappelijk Onderzoek (NWO) for the support of the FELIX Laboratory. The research leading to these results has received funding from LASERLAB-EUROPE (grant agreement no. 654148, European Union's Horizon 2020 research and innovation programme). Computations were carried out at the Georgia Tech Center for Computational Materials Science, and B.Y. and U.L. were supported by the Air Force Office for Scientific Research (AFOSR) (grant number FA9550-15-1-0519). S.M.L. is grateful to the Alexander von Humboldt Foundation for a Feodor-Lynen Scholarship, which, together with the above AFOSR grant, supported S.M.L.'s 6-month stay at the Georgia Institute of Technology during the work on this study.

References

1. Haruta, M.: Gold rush. Nature. **437**, 1098–1099 (2005)
2. Lloyd, L.: *Handbook of Industrial Catalysts*. Springer, New York, Dordrecht, Heidelberg, London (2011)
3. Farrauto, W.J., Dorazio, L., Bartholomew, C.H.: Introduction to Catalysis and Industrial Catalytic Processes. John Wiley & Sons, Hoboken, New Jersey (2016)
4. Rase, H.F.: Handbook of Commercial Catalysts Heterogeneous Catalysts. CRC Press, Boca Raton (2000)
5. Bartholomew, C.H., Farrauto, R.J.: Fundamentals of Industrial Catalytic Processes, 2nd edn. John Wiley&Sons, Hoboken, NJ (2006)
6. Stegelmann, C., Schiødt, N.C., Campbell, C.T., Stoltze, P.: Microkinetic modeling of ethylene oxidation over silver. J. Catal. **221**, 630–649 (2004)
7. Ozbek, M.O., Onal, I., van Santen, R.A.: Effect of surface and oxygen coverage on ethylene epoxidation. Top. Catal. **55**, 710–717 (2012)
8. Ozbek, M.O., Onal, I., van Santen, R.A.: Why silver is the unique catalyst for ethylene epoxidation. J. Catal. **284**, 230–235 (2011)
9. Hayashi, T., Tanaka, K., Haruta, M.: Selective vapor-phase epoxidation of propylene over Au/TiO_2 catalysts in the presence of oxygen and hydrogen. J. Catal. **178**, 566–575 (1998)
10. Lang, S.M., Bernhardt, T.M., Bakker, J.M., Yoon, B., Landman, U.: The interaction of ethylene with free gold cluster cations probed with infrared photodissociation spectroscopy. J. Phys. Condens. Matter. **30**, 504001 (2018)
11. Lyalin, A., Taketsugu, T.: Adsorption of ethylene on neutral, anionic, and cationic gold clusters. J. Phys. Chem. C. **114**, 2484–2493 (2010)
12. Kang, G.-J., Chen, Z.-X., Li, Z.: Theoretical studies of the interaction of ethylene and formaldehyde with gold clusters. J. Chem. Phys. **131**, 034710 (2009)
13. Zhao, S.Z., Li, G.Z., Liu, J.N., Ren, Y.L., Lu, W.W., Wang, J.J.: Densitiy functional study of ethylene adsorption on small gold, palladium and gold-palladium binary clusters. Eur. Phys. J. D. **68**, 254 (2014)
14. Pichugina, D.A., Lanin, S.N., Kovaleva, N.V., Lanina, K.S., Shestakov, A.F., Kuzmenko, N.E.: Effect of the structure and charge of Au_{10} clusters on adsorption of hydrocarbons. Russ. Chem. Bul. **59**, 2039–2046 (2010)
15. Pichugina, D.A., Nikolaev, S.A., Mukhamedzyanova, D.F., Kuzmenko, N.E.: Quantum-chemical modeling of ethylene and acetylene adsorption on gold clusters. Russ. J. Phys. Chem. A. **88**, 959–964 (2014)
16. Tsipis, A.C.: Unveiling the nature of binding interactions of acetylene and ethylene with triangular coinage metal clusters: a DFT computational study. Organometallics. **29**, 354–363 (2010)
17. Sanchez, A., Abbet, S., Heiz, U., Schneider, W.-D., Häkkinen, H., Barnett, R.N., Landman, U.: When gold is not noble: nanoscale gold catalysts. J. Phys. Chem. A. **103**, 9573–9578 (1999)
18. Socaciu, L.D., Hagen, J., Bernhardt, T.M., Wöste, L., Heiz, U., Häkkinen, H., Landman, U.: Catalytic CO oxidation by free Au_2^-: experiment and theory. J. Am. Chem. Soc. **125**, 10437–10445 (2003)
19. Häkkinen, H., Landman, U.: Gas-phase catalytic oxidation of CO by Au_2^-. J. Am. Chem. Soc. **123**, 9704–9705 (2001)
20. Lang, S.M., Bernhardt, T.M., Barnett, R.N., Landman, U.: Temperature-tunable selective catalytic oxidation of methane on free Au_2^+: formaldehyde vs. ethylene formation. J. Phys. Chem. C. **115**, 6788–6795 (2011)
21. Lang, S.M., Bernhardt, T.M., Barnett, R.N., Yoon, B., Landman, U.: Hydrogen-promoted oxygen activation by free gold cluster cations. J. Am. Chem. Soc. **131**, 8939–8951 (2009)
22. Gao, W., Chen, X.F., Li, J.C., Jiang, Q.: Is Au_{55} or Au_{38} cluster a threshold catalyst for styrene epoxidation? J. Phys. Chem. C. **114**, 1148–1153 (2010)
23. Outka, D.A., Madix, R.J.: Bronsted basicity of atomic oxygen on the Au(110) surface: reactions with methanol, acetylene, water, and ethylene. J. Am. Chem. Soc. **109**, 1708–1714 (1987)
24. Patterson, M.L., Weaver, M.J.: Adsorption and oxidation of ethylene at gold electrodes as examined by surface-enhanced Raman spectroscopy. J. Phys. Chem. **89**, 1331–1334 (1985)
25. Šebera, J., Hoffmannová, H., Krtil, P., Samec, Z., Záliš, S.: Electrochemical and density functional studies of the catalytic ethylene oxidation on nanostructured Au electrodes. Catal. Today. **158**, 29–34 (2010)
26. Rojluechai, S., Chavadej, S., Schwank, J.W., Meeyoo, V.: Catalytic activity of ethylene oxidation over Au, Ag and Au–Ag catalysts: support effect. Catal. Commun. **8**, 57–64 (2007)
27. Torres, D., Illas, F.: On the performance of Au(111) for ethylene epoxidation: a density functional study. J. Phys. Chem. B. **110**, 13310–13313 (2006)
28. Chen, H.-T., Chang, J.-G., Ju, S.-P., Chen, H.-L.: Ethylene epoxidation on a Au nanoparticle versus a Au(111) surface: a DFT study. J. Phys. Chem. Lett. **1**, 739–742 (2010)
29. Kokalj, A., Gava, P., de Gironcoli, S., Baroni, S.: What determines the catalyst's selectivity in the ethylene epoxidation reaction. J. Catal. **254**, 304–309 (2008)
30. Kobayashi, H., Shimodaira, Y.: Density functional study of propylene oxidation on Ag and Au surfaces. Comparison to ethylene oxidation. THEOCHEM J. Mol. Struct. **762**, 57–67 (2006)
31. Nakatsuji, H., Hu, Z.-M., Nakai, H., Ikeda, K.: Activation of O_2 on Cu, Ag, and Au surfaces for the epoxidation of ethylene: dipped adcluster model study. Surf. Sci. **387**, 328–341 (1997)
32. Lee, C.-C., Chen, H.-T.: Adsorption and reaction of C_2H_4 and O_2 on a Nanosized gold cluster: a computational study. J. Phys. Chem. A. **119**, 8547–8555 (2015)
33. Liu, X., Yang, Y., Chu, M., Duan, T., Meng, C., Han, Y.: Defect stabilized gold atoms on graphene as potential catalysts for ethylene epoxidation: a first-principles investigation. Catal. Sci. Technol. **6**, 1632–1641 (2016)
34. Chen, H.-T., Chan, C.-W.: Promoting ethylene epoxidation on gold nanoclusters: self and CO induced O_2 activation. Phys. Chem. Chem. Phys. **17**, 22336–22341 (2015)
35. Lyalin, A., Taketsugu, T.: Cooperative adsorption of O_2 and C_2H_4 on small gold clusters. J. Phys. Chem. C. **113**, 12930–12934 (2009)
36. Lyalin, A., Taketsugu, T.: Reactant-promoted oxygen dissociation on gold clusters. J. Phys. Chem. Lett. **1**, 1752–1757 (2010)

37. Bakker, J.M., Lapoutre, V.J.F., Redlich, B., Oomens, J., Sartakov, B.G., Fielicke, A., von Helden, G., Meijer, G., van der Meer, A.F.G.: Intensity-resolved IR multiple photon ionization and fragmentation of C_{60}. J. Chem. Phys. **132**, 074305 (2010)
38. Lang, S.M., Bernhardt, T.M., Bakker, J.M., Yoon, B., Landman, U.: Selective C-H bond activation of ethane by free gold clusters. Int. J. Mass Spectrom. **435**, 241–250 (2019)
39. Kresse, G., Hafner, J.: Ab. initio molecular dynamics for liquid metals. Phys. Rev. B. **47**, 558–561 (1993)
40. Kresse, G., Hafner, J.: Ab initio molecular-dynamics simulation of the liquid-metal -amorphous-semiconductor transition in germanium. Phys. Rev. B. **49**, 14251–14269 (1994)
41. Kresse, G., Furthmüller, J.: Efficient iterative schemes for ab initio total-energy calculations using a plane-wave basis set. Phys. Rev. B. **54**, 11169–11185 (1996)
42. Kresse, G., Furthmüller, J.: Efficiency of ab-initio total energy calculations for metals and semiconductors using a plane-wave basis set. Comput. Mater. Sci. **6**, 15–50 (1996)
43. Kresse, G., Joubert, D.: From ultrasoft pseudopotentials to the projector augmented-wave method. Phys. Rev. B. **59**, 1758–1775 (1999)
44. Perdew, J.P., Burke, K., Ernzerhof, M.: Generalized gradient approximation made simple. Phys. Rev. Lett. **77**, 3865–3868 (1996)
45. Makov, G., Payne, M.C.: Periodic boundary conditions in ab initio calculations. Phys. Rev. B. **51**, 4014–4022 (1995)
46. Cordero, B., Gómez, V., Platero-Prats, A.E., Revés, M., Echeverría, J., Cremades, E., Barragán, F., Alvarez, S.: Covalent radii revisited. Dalton Trans. **2008**, 2832–2838 (2008)
47. Giannozzi, P., Baroni, S.: Vibrational and dielectric properties of C_{60} from density-functional perturbation theory. J. Chem. Phys. **100**, 8537–8539 (1994)
48. Baroni, S., de Gironcoli, S., Dal Corso, A., Giannozzi, P.: Phonons and related crystal properties from density-functional perturbation theory. Rev. Mod. Phys. **73**, 515–561 (2001)
49. Yoon, B., Häkkinen, H., Landman, U.: Interaction of O_2 with gold clusters: molecular and dissociative adsorption. J. Phys. Chem. A. **107**, 4066–4071 (2003)
50. Bernhardt, T.M.: Gas-phase kinetics and catalytic reactions of small silver and gold clusters. Int. J. Mass Spectrom. **243**, 1–29 (2005)
51. Cox, D.M., Brickman, R., Creegan, K., Kaldor, A.: Gold clusters: reactions and deuterium uptake. Z. Phys. D. **19**, 353–355 (1991)
52. Lee, T.H., Ervin, K.M.: Reactions of copper group cluster anions with oxygen and carbon monoxide. J. Chem. Phys. **98**, 10023–10031 (1994)
53. Salisbury, B.E., Wallace, W.T., Whetten, R.L.: Low-temperature activation of molecular oxygen by gold clusters: a stoichiometric process correlated to electron affinity. Chem. Phys. **262**, 131–141 (2000)
54. Hagen, J., Socaciu, L.D., Elijazyfer, M., Heiz, U., Bernhardt, T.M., Wöste, L.: Coadsorption of CO and O_2 on small free gold cluster anions at cryogenic temperatures: model complexes for catalytic CO oxidation. Phys. Chem. Chem. Phys. **4**, 1707–1709 (2002)
55. Stolcic, D., Fischer, M., Ganteför, G., Kim, Y.D., Sun, Q., Jena, P.: Direct observation of key reaction intermediates on gold clusters. J. Am. Chem. Soc. **125**, 2848–2849 (2003)
56. Woodham, A.P., Meijer, G., Fielicke, A.: Activation of molecular oxygen by anionic gold clusters. Angew. Chem. Int. Ed. **51**, 4444 (2012)
57. Cox, D.M., Brickman, R., Creegan, K., Kaldor, A.: Studies of the chemical properties of size selected metal clusters: kinetics and saturation. Mat. Res. Soc. Symp. Proc. **206**, 43 (1991)
58. Koszinowski, K., Schröder, D., Schwarz, H.: Additivity effects in the reactivities of bimetallic cluster ions $Pt_mAu_n^+$. Chem. Phys. Chem. **4**, 1233–1237 (2003)
59. Bürgel, C., Reilly, N.M., Johnson, G.E., Mitrić, R., Kimble, M.L., Castleman Jr., A.W., Bonačić-Koutecký, V.: Influence of charge state on the mechanism of CO oxidation on gold clusters. J. Am. Chem. Soc. **130**, 1694–1698 (2008)
60. Lang, S.M., Bernhardt, T.M.: Cooperative and competitive coadsorption of H_2, O_2, and N_2 on Au_x^+ (x = 3,5). J. Chem. Phys. **131**, 024310 (2009)
61. Woodham, A.P., Fielicke, A.: Superoxide formation on isolated cationic gold clusters. Angew. Chem. Int. Ed. **53**, 6554–6557 (2014)
62. Johnson, G.E., Reilly, N.M., Tyo, E.C., Castleman Jr., A.W.: Gas-phase reactivity of gold oxide cluster cations with CO. J. Phys. Chem. C. **112**, 9730–9736 (2008)
63. NIST Chemistry Webbook: *Nist Standard Reference Database*, 69th edn. National Institute of Standards and Technology, Gaithersburg MD http://webbook.nist.gov
64. Lide, D.R.: Handbook of Chemistry and Physics, 76th edn. CRC Press, Boca Raton, FL (1995)
65. Yoon, B., Koskinen, P., Huber, B., Kostko, O., von Issendorff, B., Häkkinen, H., Moseler, M., Landman, U.: Size-dependent structural evolution and chemical reactivity of gold clusters. ChemPhysChem. **8**, 157–161 (2007)
66. Torres, M.B., Fernández, E.M., Balbás, L.C.: Theoretical study of oxygen adsorption on pure Au_{n+1}^+ and doped MAu_n^+ cationic gold clusters for M= Ti, Fe and n = 3-7. J. Phys. Chem. A. **112**, 6678–6689 (2008)
67. Varganov, S.A., Olson, R.M., Gordon, M.S., Metiua, H.: The Interaction of Oxygen with Small Gold. Clusters. **119**, 2531–2537 (2003)
68. Sun, Q., Jena, P., Kim, Y.D., Fischer, M., Ganteför, G.: Interactions of Au cluster anions with oxygen. J. Chem. Phys. **120**, 6510–6515 (2004)
69. Mills, G., Gordon, M.S., Metiu, H.: Oxygen adsorption on Au clusters and a rough Au(111) surface: the role of surface flatness, electron confinement, excess electrons, and band gap. J. Chem. Phys. **118**, 4198–4205 (2003)
70. Mills, G., Gordon, M.S., Metiu, H.: The adsorption of molecular oxygen on neutral and negative Au_n clusters (n = 2–5). Chem. Phys. Lett. **359**, 493–499 (2002)
71. Ding, X., Li, Z., Yang, J., Hou, J.G., Zhu, Q.: Adsorption energies of molecular oxygen on Au clusters. J. Chem. Phys. **120**, 9594–9594 (2004)
72. Okumura, M., Kitagawa, Y., Haruta, M., Yamaguchi, K.: The interaction of neutral and charged Au clusters with O_2, CO and H_2. Appl. Catal. A: General. **291**, 37–44 (2005)
73. Woodham, A.P., Meijer, G., Fielicke, A.: Charge separation promoted activation of molecular oxygen by neutral gold clusters. J. Am. Chem. Soc. **135**, 1727–1730 (2013)